

Mass functions and structure of the young open cluster NGC 6611

C. Bonatto¹, J. F. C. Santos Jr.², and E. Bica¹

¹ Universidade Federal do Rio Grande do Sul, Instituto de Física, CP 15051, Porto Alegre 91501-970, RS, Brazil
e-mail: charles@if.ufrgs.br

² Universidade Federal de Minas Gerais, ICEx, Departamento de Física, CP 702, Belo Horizonte 30162-970, MG, Brazil

Received 31 January 2005 / Accepted 9 September 2005

ABSTRACT

We use J , H and K_s 2MASS photometry to study colour–magnitude (CMDs) and colour–colour diagrams, structure and mass distribution in the ionizing open cluster NGC 6611. Reddening variation throughout the cluster region is taken into account followed by field-star decontamination of the CMDs. Decontamination is also applied to derive the density profile and luminosity functions in the core, halo and overall (whole cluster) regions. The field-star decontamination showed that the lower limit of the main sequence (MS) occurs at $\approx 5 M_\odot$. Based on the fraction of K_s excess stars in the colour–colour diagram we estimate an age of 1.3 ± 0.3 Myr which is consistent with the presence of a large number of pre-main sequence (PMS) stars. The distance from the Sun was estimated from known O V stars in the cluster area and the turn-on stars connecting the PMS and MS, resulting in $d_\odot = 1.8 \pm 0.5$ kpc. The radial density distribution including MS and PMS stars is fitted by a King profile with a core radius $R_{\text{core}} = 0.70 \pm 0.08$ pc. The cluster density profile merges into the background at a limiting radius $R_{\text{lim}} = 6.5 \pm 0.5$ pc. From the field-star subtracted luminosity functions we derive the mass functions (MFs) in the form $\phi(m) \propto m^{-(1+\chi)}$. In the halo and through the whole cluster the MFs have slopes $\chi = 1.52 \pm 0.13$ and $\chi = 1.45 \pm 0.12$, respectively, thus slightly steeper than Salpeter’s IMF. In the core the MF is flat, $\chi = 0.62 \pm 0.16$, indicating some degree of mass segregation since the cluster age is a factor ~ 2 larger than the relaxation time. Because of the very young age of NGC 6611, part of this effect appears to be related to the molecular cloud-fragmentation process itself. We detect 362 ± 120 PMS stars. The total observed mass including detected MS (in the range 5–85 M_\odot) and PMS stars amounts to $\sim 1600 M_\odot$, thus more massive than the Trapezium cluster. Compared to older open clusters of different masses, the overall NGC 6611 fits in the relations involving structural and dynamical parameters. However, the core is atypical in the sense that it looks like an old/dynamically evolved core. Again, part of this effect must be linked to formation processes.

Key words. Galaxy: open clusters and associations: individual: NGC 6611 – Galaxy: structure

1. Introduction

The distribution of stellar masses at star-cluster birth is a complex process not yet fully understood. Recent observations of the stellar content of star-forming regions in molecular clouds, rich star clusters and the Galactic field suggest that the initial mass function (IMF) has similar properties in these very different environments (Kroupa 2002). This seems to indicate that the initial distribution of stellar masses should depend only on the process of molecular cloud fragmentation, and that the fragmentation would have to produce similar IMFs despite very different initial conditions, a physical process which still lacks a better description (Kroupa 2002). In this sense, detailed analysis of the spatial structure and stellar-mass distribution in young star clusters may shed light on this issue. A suitable target for this kind of study is the young open cluster NGC 6611, which is responsible for the ionization of the H II region Sh2-49 (Sharpless 1959), aka Gum 83 (Gum 1955) or RCW 165 (Rodgers et al. 1960) as seen in the optical, or W 37 (Westerhout 1958) in the radio.

The open cluster NGC 6611 (M 16, Mel-198, Cr 375, OCl 54 – Alter et al. 1970) consists of a system of early-type stars embedded in emission nebulosity (The Eagle Nebula) with spatially variable dust attenuation in the optical range. Structurally the region shows some nebulosity features, the so-called elephant trunks (the “Pillars of Creation”, Hester et al. 1996), at the tips of which new-born stars start to be visible.

The cluster is located at $\ell \approx 17^\circ$ and $b \approx 0.8^\circ$, in the Sagittarius spiral arm (Georgelin & Georgelin 1970), a region presenting conspicuous dense dust clouds. The whole region is an active site where star-formation processes seem to occur giving birth to low to high-mass stars (Kroupa 2004). Evidence has been presented in recent years that NGC 6611 shows an extremely flat MF (e.g. Sagar & Joshi 1979; Sagar et al. 1986; Hillenbrand et al. 1993; Massey et al. 1995). The distance of NGC 6611 is dependent on the extinction law but several works constrain it to $d_\odot = 2.3 \pm 0.3$ kpc (Thé et al. 1990; Hillenbrand et al. 1993; Belikov et al. 1999). The cluster stars

have been observed in evolutionary stages which are not reconcilable with a single age system (de Winter et al. 1997). Also, isochrone age determinations are ambiguous for such young clusters because of the lack of constraints in the CMD morphology. However, several studies show that the cluster is certainly younger than 10 Myr with the youngest members still being formed (e.g. Hillenbrand et al. 1993; de Winter 1997; Belikov et al. 2000). NGC 6611 presents a significant number of PMS stars. de Winter et al. (1997) revised the subject of PMS membership and related issues by studying PMS candidates individually via photometry and spectroscopy. They find that the sample objects are not coeval, with an age spread of ≈ 6 Myr being necessary to explain the cluster stellar content.

Our main goals with the present work are (i) carry out a detailed analysis of the spatial structure of NGC 6611, (ii) analyze the spatial variation of the cluster MFs, (iii) derive properties of the MS and PMS stars, and (iv) infer on the dynamical state of this very young open cluster. For the sake of spatial and photometric uniformity, we employ J , H and K_S 2MASS¹ photometry. The 2MASS Point Source Catalogue (PSC) is uniform reaching relatively faint magnitudes covering nearly all the sky, allowing a proper background definition even for clusters with large angular sizes (e.g. Bonatto et al. 2004; Bonatto et al. 2004).

This paper is organized as follows. In Sect. 2 we condense previous results on NGC 6611. In Sect. 3 we present the 2MASS data, correct the photometry for differential reddening, subtract the field-star contamination and analyze the CMDs and colour–colour diagrams. In Sect. 4 we discuss the cluster structure. In Sect. 5 we derive LFs and MFs and discuss stellar content properties. In Sect. 6 we compare NGC 6611 with nearby, older open clusters and discuss dynamical states. Finally, concluding remarks are given in Sect. 7.

2. The young open cluster NGC 6611

The equatorial young open cluster NGC 6611 is included in the Ser OB 1 association and the W 37 molecular cloud. It is part of a larger sequence of star-forming events which have just begun in the region and are still embedded in the molecular cloud (Hillenbrand et al. 1993). The cluster contains 8 O V-stars (Bosch et al. 1999).

The first comprehensive photometric study on this object was carried out by Walker (1961) who obtained UBV photoelectric and photographic observations of NGC 6611 limited at $V = 16.7$. He found that in the southern part of the region the colour excess is relatively small, $E(B - V) = 0.6$, while to the north the reddening increases irregularly reaching $E(B - V) = 1.73$. Stars above the MS were considered possible members in the gravitational contraction phase. He derived an age of 1.8 Myr based on the analysis of 532 probable member stars.

Sagar & Joshi (1979) derived a distance to the Sun $d_\odot = 3.2 \pm 0.3$ kpc, an age in the range 3.0–5.5 Myr, and observed an extremely flat luminosity function in this open cluster.

Based on photoelectric UBV photometry, Sagar et al. (1986) derive a flat MF with a slope $\chi \approx -0.2$ for stars in the mass range $9 \leq m(M_\odot) \leq 70$.

By means of photometric observations over the range from 0.3 to $3.7 \mu\text{m}$ Chini & Wargau (1990) provide evidence of an abnormal extinction law only at wavelengths shorter than $0.55 \mu\text{m}$. They conclude that all PMS stars previously identified by Walker (1961) present reddening due to normal dust, therefore suggesting that they are foreground objects.

Hillenbrand et al. (1993) combined CCD UBV observations with near-infrared JHK ones to establish a theoretical HR diagram for the cluster, from which they conclude that NGC 6611 is actively forming $3\text{--}8 M_\odot$ stars. Using the optical data they infer from a spatial coverage of $\approx 1600''^2$ an overall MS MF slope of $\chi = 0.1\text{--}0.3$ in the mass range $5 \leq m(M_\odot) \leq 85$. It is worth noting that only 4 stars have masses between 40 and $85 M_\odot$, for which they derive an age of 2 ± 1 Myr. They also present evidence that one $30 M_\odot$ star has been formed ~ 6 Myr ago. They derive $d_\odot = 2.0 \pm 0.1$ kpc.

By constructing new HR diagrams from the data published by Hillenbrand et al. (1993) and applying a different mass calibration, Massey et al. (1995) derived an age in the range 1–5 Myr, $\chi = -0.3 \pm 0.2$, and a stellar density of $\rho = 5.4 \times 10^4 \text{ kpc}^{-2}$ for stars above $10 M_\odot$.

Belikov et al. (1999) analyzed the spatial and proper motion distribution of cluster stars, assuming a normal distribution for the spatial velocities. They derived a distance to the Sun $d_\odot = 2.14 \pm 0.10$ kpc and obtained spatial dispersions of $\sigma_{XY}^{\text{core}} = 1.20'$ and $\sigma_{XY}^{\text{corona}} = 4.77'$, respectively for the core and corona subsystems in NGC 6611. They used the same data to measure the differential reddening throughout the cluster area.

Belikov et al. (2000) studied NGC 6611 based on a compilation of photographic, photoelectric and CCD optical (UBV) observations covering a circular area of $45.6'$ in diameter centered on NGC 6611. They present radial profiles of the star density distribution in different azimuthal sectors. Small differences found between the density of the north-west and south-east sectors were attributed to irregularities of the absorption due to interstellar dust rather than to stellar density fluctuations. The south-east sector of the cluster is less affected by dust than the north-west one. The total radial density distribution allowed them to conclude that virtually no cluster members are present beyond the edge of the cluster corona, at $3\sigma_{XY}^{\text{corona}} = 14.3'$. They derive an age of 6 Myr for NGC 6611. Based on the number frequency of member stars in the range $2.1 \leq m(M_\odot) \leq 85$ they infer a flat MF slope, $\chi = 0.2$.

Tadross et al. (2002) presented an analysis of UBV CCD observations intending to derive morphological parameters for a large sample of open clusters. For NGC 6611 they obtained a colour excess $E(B - V) = 0.68$, $d_\odot \approx 1.6$ kpc, age ≈ 3.2 Myr, linear diameter $D = 3.6$ pc, Galactocentric distance $d_{GC} = 6.94$ kpc, number of member stars $N_* = 282$, and a total mass of $m_{\text{MS+PMS}} = 435 M_\odot$.

The presence of significant numbers of PMS stars in NGC 6611 has been confirmed by means of the observation of

¹ The Two Micron All Sky Survey, All Sky data release (Skrutskie et al. 1997), available at <http://www.ipac.caltech.edu/2mass/releases/allsky/>

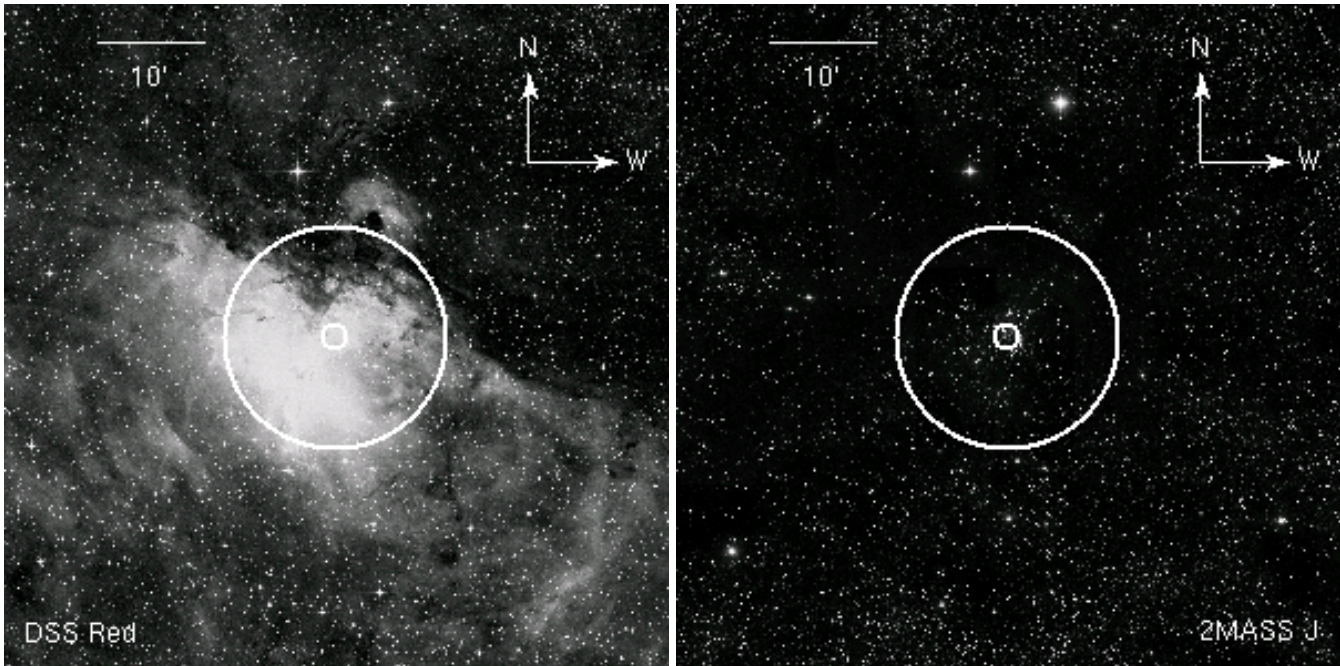


Fig. 1. *Left panel:* XDSS *R* image. *Right panel:* 2MASS *J* image. The area covered in both images is $1^\circ \times 1^\circ$. The small circle at the center of each image indicates the core, and the large one indicates the size of NGC 6611 (limiting radius).

a large number of emission-line stars and IR disk signatures (Hillenbrand et al. 1993; Massey et al. 1995), which is an expected population in such a young cluster. Recently Oliveira et al. (2005) obtained *IZJHKL'* photometry aiming at identifying PMS stars in NGC 6611. Their Fig. 2 shows the CMDs $I \times (I - Z)$ for the central area ($7' \times 6'$) and for a control field $16'$ away from the cluster center. The PMS population, defined within $12 < I < 19$, corresponding to the mass range $0.4 < m(M_\odot) < 7$, stands out in the central area and decreases significantly towards the control field. The MS population does not show such trend, its spatial distribution remaining apparently constant throughout the fields.

In the left panel of Fig. 1 we provide an *R* XDSS image encompassing an area of $1^\circ \times 1^\circ$ centered on NGC 6611, extracted from the Canadian Astronomy Data Centre (CADC²). In the right panel we show the corresponding 2MASS *J* image. The stark contrast between the *R* and *J* images reflects primarily the effect of the $H\alpha$ emission in the *R* band and how dust is much more penetrable in the near-infrared bands. Thus, the analysis of NGC 6611 and its outskirts with near-infrared data is naturally justified because it allows access to low-mass stars with moderate aperture telescopes. In this sense, Hillenbrand et al. (1993) investigated NGC 6611 by means of deep near-infrared observations covering a $15' \times 15'$ area with useful limits of $J = 16$, $H = 14.5$ and $K = 13.5$, similar to those of 2MASS.

According to the WEBDA³ open cluster database (Mermilliod 1996), the central coordinates of NGC 6611 are (J2000) $\alpha = 18^{\text{h}}18^{\text{m}}48^{\text{s}}$, and $\delta = -13^\circ48'24''$. However, the corresponding radial density profile (Sect. 4) presented a

dip for $R = 0'$. Accordingly, we searched for a new center by examining histograms for the number of stars in $1'$ bins of right ascension and declination. The resulting coordinates which maximize the density of stars at the center are (J2000) $\alpha = 18^{\text{h}}18^{\text{m}}40.8^{\text{s}}$, and $\delta = -13^\circ47'24.0''$, corresponding to $\ell = 16.95^\circ$ and $b = 0.83^\circ$. In what follows we refer to these optimized coordinates as the center of NGC 6611. WEBDA gives a colour excess of $E(B - V) = 0.768$, distance to the Sun $d_\odot = 1.75$ kpc, and age ≈ 7.6 Myr.

3. Photometric parameters from 2MASS data

The VizieR⁴ tool was used to extract *J*, *H* and K_S 2MASS photometry of the stars present in a circular area with radius $R = 60'$ centered on the optimized coordinates described in the previous section. The faint-magnitude limit of the extracted stars is brighter than that corresponding to the 99.9% Point Source Catalogue Completeness Limit⁵, $J = 15.8$, $H = 15.1$ and $K_S = 14.3$, respectively.

As a first step in the investigation of NGC 6611 we use the 2MASS data to examine in Fig. 2 the distribution of stars in the area surrounding the cluster. Each panel depicts the number of stars brighter than $J = 15.8$ in strips of $5'$ width in declination (left panels) and right ascension (right panels) with respect to the optimized cluster center. The rather concentrated structure of NGC 6611 is apparent in panels e and f. Within uncertainties the cluster appears to be spatially asymmetric, being more extended in right ascension (apparent diameter $D_\alpha \sim 21'$,

⁴ <http://vizier.u-strasbg.fr/viz-bin/VizieR?-source=II/246>

⁵ According to the Level 1 Requirement, according to http://www.ipac.caltech.edu/2mass/releases/allsky/doc/sec6_5a1.html

² <http://cadwww.dao.nrc.ca/>

³ <http://obswww.unige.ch/webda>

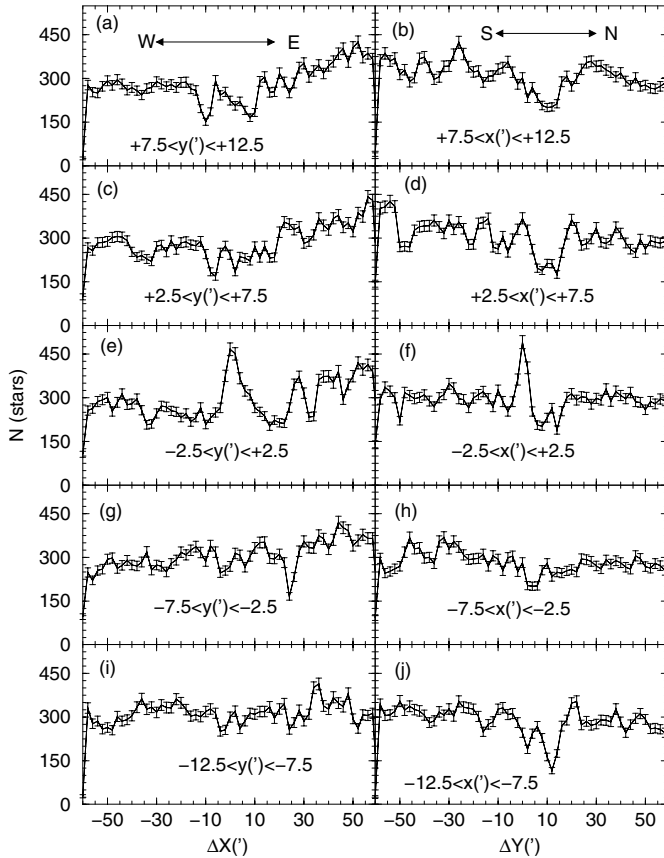


Fig. 2. Spatial distribution of the number of stars (brighter than $J = 15.8$) around the central position of NGC 6611. The density of stars increases to the East and South. 1σ Poisson errors are shown.

(panel e) than in declination ($D_\delta \sim 12'$), (panel f). The spatial distribution of stars around the cluster is non-uniform, increasing significantly above the 1σ Poisson errors towards the East (panels a, c, e and g) and less markedly to the South (panels b and d). Part of this non-uniformity can be accounted for by differential reddening, which is important throughout the cluster area (Belikov et al. 1999).

3.1. Spatial variation of reddening

Because of the low Galactic latitude ($b = 0.83^\circ$), the field of NGC 6611 presents significant field-star contamination. This can be seen in the left panels of Fig. 3 where we show the observed $J \times (J - H)$ CMDs of three consecutive circular regions ($\Delta R = 3'$) centered on NGC 6611. Besides conspicuous MS stars, the integrated CMD up to $R = 9'$ (bottom panel) presents important field-star contamination.

As discussed in Belikov et al. (1999), the spatial field of NGC 6611 is critically affected by differential reddening with important variations both in $E(B - V)$ and R_V in areas separated by distances as small as $\sim 2'$. They present $E(B - V)$ and R_V values derived from spectroscopy and proper motion of cluster stars in $2' \times 2'$ cells covering an area of about $40' \times 36'$ centered on NGC 6611. Note that $E(B - V)$ in each cell corresponds to the absolute reddening value.

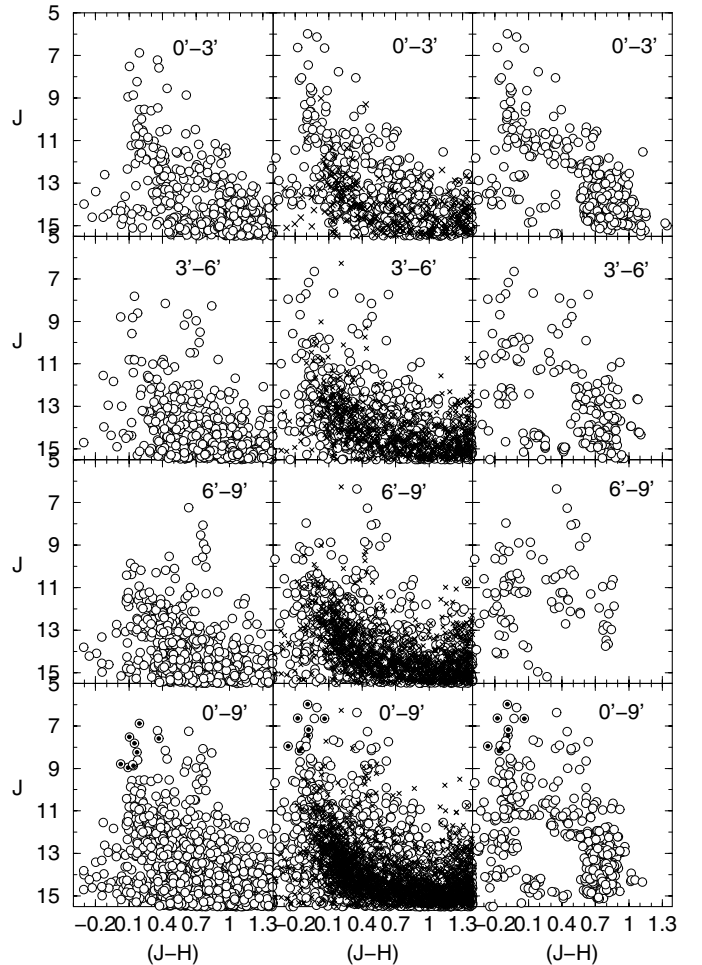


Fig. 3. $J \times (J - H)$ CMDs of the central $9'$ of NGC 6611. *Left panels:* observed photometry. *Middle panels:* reddening-corrected CMDs according to Belikov et al. (1999). *Right panels:* reddening-corrected and field-star decontaminated CMDs. Note the extended MS and conspicuous PMS population, which is restricted essentially to the central $6'$. Field stars are shown as x in the middle panels. Filled circles in the *bottom panels:* O V stars from Bosch et al. (1999).

We applied the above procedure to produce reddening-corrected 2MASS photometry for all stars in each cell to yield a total region reaching $R \approx 23'$ from the center of NGC 6611. In the vacant cells we followed their suggestion and adopted the average values of $E(B - V)$ and R_V . For reddening and absorption transformations in the 2MASS bands we use the relations $A_J = 0.276 \times R_V E(B - V)$, $A_H = A_J - 0.33 E(B - V)$ and $A_{K_s} = A_J - 0.49 E(B - V)$, according to Dutra et al. (2002, and references therein).

The resulting reddening-corrected CMDs are shown in the middle panels of Fig. 3. Comparison of the reddening-corrected CMDs with the observed ones shows that the average colour-excess throughout the cluster area is $\langle E(J - H) \rangle = 0.25$, corresponding to $\langle E(B - V) \rangle = 0.8$.

3.2. Field-star decontamination

Finally, to uncover the intrinsic CMD morphology we apply a field-star decontamination procedure. Because of the spatial limitation on the useful area caused by the differential-reddening correction (Sect. 3.1), we consider as offset field the ring located at $17' \leq R \leq 22'$. This area is large enough to produce statistical representativity of the field stars, both in magnitude and colours.

To illustrate the amount and colour–magnitude distribution of the contamination in the area of NGC 6611 we plot in the middle panels of Fig. 3 the corresponding (same area) field-star contributions taken from rings with external radius at $22'$. As a consequence we can see that most of the faint stars – in particular those mimicking a low-MS – are in fact field-stars.

Based on the spatial number-density of stars in the offset field, the decontamination procedure estimates the number of field stars which within the 1σ Poisson fluctuation should be present in the cluster field. The observed CMD is then divided in colour/magnitude cells from which stars are randomly subtracted in a number consistent with the expected number of field stars in the same cell. The dimensions of the colour/magnitude cells can be subsequently changed so that the total number of stars subtracted throughout the whole cluster area matches the expected one, within the 1σ Poisson fluctuation. Since the field stars are taken from an external annulus of fixed dimensions, corrections are made for the different solid angles of cluster and offset field. This procedure can be applied to the cluster region as a whole or internal regions as well. Note that because this procedure actually excludes stars from the original files – thus artificially changing both the radial distribution of stars and the LF – we use it only for the sake of uncovering the intrinsic CMD morphology.

The resulting field-star decontaminated (differential-reddening corrected) CMDs are shown in the right panels of Fig. 3. As expected, most of the faint-star distribution was subtracted by the decontamination procedure. The central region ($0' \leq R \leq 3'$) presents an extended, vertical MS reaching from $J \approx 11.5$ to $J \approx 5.5$ which reflects the young age of NGC 6611. This region also presents a conspicuous population of PMS stars ($0.54 \leq (J - H) \leq 1.1$) which extends essentially up to $R \approx 6'$. The entry point (turn-on stars) of the PMS into the MS occurs at $J \approx 11.1$. The region $6' \leq R \leq 9'$ is sparsely populated by cluster stars, with a small fraction of MS and PMS stars still discernible.

3.3. Age

Deriving a precise age for clusters younger than ~ 10 Myr by means of isochrone fit is a difficult task because of the nearly-vertical MS and lack of post-MS stars. As a consequence of the scarcity of observational constraints in the CMD, several age-solutions are possible. In the case of NGC 6611, the CMD (Fig. 3) can be acceptably fitted with isochrones with ages up to 10 Myr. In the present case we use the set of solar-metallicity isochrones of Padova (Girardi et al. 2002) computed with the

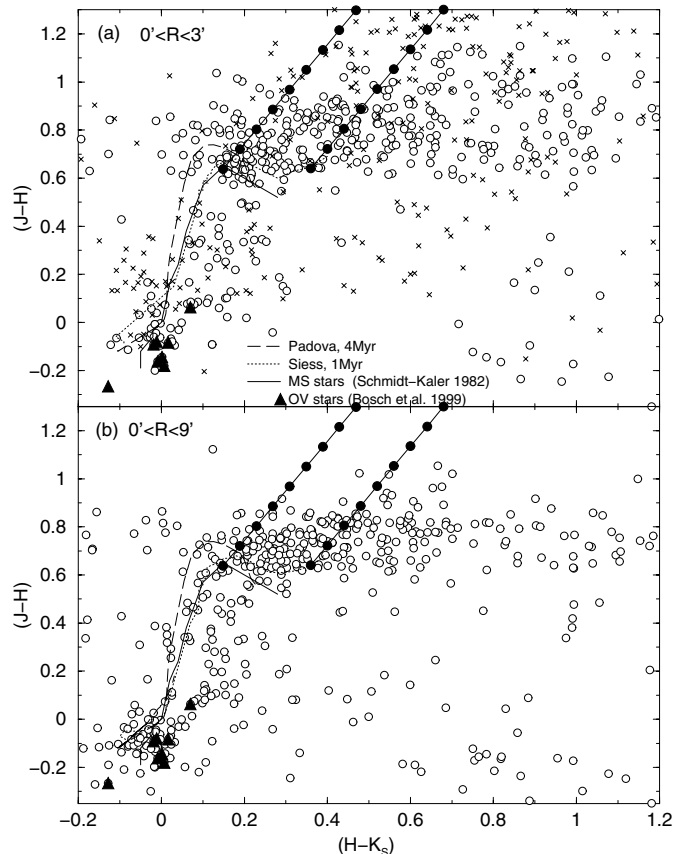


Fig. 4. $(H - K_S) \times (J - H)$ diagram of the central $3'$ (Panel a)) and $9'$ (Panel b)) of NGC 6611. Dashed line: 4 Myr Padova isochrone. Dotted line: 1 Myr sequence of PMS stars (Siess et al. 2000). Solid line: MS stars from Schmidt-Kaler (1982). Filled triangles: OV stars (Bosch et al. 1999). Filled circles: reddening vectors; $\Delta E(B - V) = 0.25$ between 2 consecutive circles. The corresponding field stars are shown in Panel a) as “x”. Both diagrams were produced after field-star decontamination.

2MASS J , H and K_S filters⁶. The 2MASS transmission filters produced isochrones very similar to the Johnson ones, with differences of at most 0.01 in $(J - H)$ (Bonatto et al. 2004).

On the other hand, properties of young/embedded objects, in particular the age, can be alternatively inferred by means of infrared colour–colour diagrams (e.g. Lada et al. 1996). The fraction of stars with K_S excess in embedded clusters is an age indicator (e.g. Lada et al. 1996; Soares & Bica 2002) in the sense that larger fractions correspond to younger evolutionary stages. In Fig. 4 we show the $(H - K_S) \times (J - H)$ diagram of the central $3'$ (Panel a) and $9'$ (Panel b) of NGC 6611. Both diagrams were produced after differential-reddening correction and field-star decontamination. To compare stars in different evolutionary stages we show in Panel a the loci occupied by MS stars according to the youngest Padova isochrone (4 Myr) and to those of Schmidt-Kaler (1982). The 1 Myr sequence of PMS stars (Siess et al. 2000), and the loci of the OV stars with available spectroscopic data of Bosch et al. (1999) are shown

⁶ http://pleiadi.pd.astro.it/isoc_photsys.01/isoc_photsys.01.html

as well. Extinction effects can be estimated by the reddening vectors.

For NGC 6611 we measured within $R \leq 3'$ a fraction of $f_{\text{exc}} = 0.54 \pm 0.05$ of K_S excess stars. Considering uncertainties this value is intermediate between those of the ρ Ophiuchi cluster ($f_{\text{exc}} = 0.5\text{--}0.7$ – Greene & Young 1992; Strom et al. 1995) with an age of 1 Myr or less (Greene & Meyer 1995) and that of the Taurus Dark Nebula group ($f_{\text{exc}} = 0.5$ – Kenyon & Hartmann 1995) with an age of 1.5 Myr. Based on this we estimate an age of 1.3 ± 0.3 Myr for NGC 6611. These values are similar to those of Trapezium, NGC 2327 cluster and BRC 27 cluster (Soares & Bica 2002).

This estimate is consistent with (i) the presence of a significant population of PMS (e.g. Walker 1961; Hillenbrand et al. 1993; Massey et al. 1995; Oliveira et al. 2005), (ii) the fraction of $\sim 58\%$ of PMS having circumstellar discs (e.g. Hillenbrand et al. 1993; Massey et al. 1995; Oliveira et al. 2005), and (iii) the fact that NGC 6611 is ionizing the H II region Sh2-49 (e.g. Bosch et al. 1999; Hillenbrand et al. 1993).

3.4. Distance from the Sun

Similarly to the age, the lack of evolved features in the CMD of NGC 6611 precludes a precise distance determination based directly on isochrone fit. In this sense we will derive the distance of NGC 6611 from the Sun using two independent methods. Bosch et al. (1999) derived spectroscopic data of 8 MS O member stars (which are identified in the bottom panels of Fig. 3). Each O V star was corrected for reddening according to the corresponding cell $E(B - V)$ and R_V values in Belikov et al. (1999). From these stars we derive an absolute average distance modulus of $(m - M)_O = 11.39 \pm 0.46$, corresponding to a distance from the Sun $d_\odot = 1.92 \pm 0.45$ kpc. We use this value to set the 4 Myr Padova isochrone in the reddening-corrected, field-star decontaminated CMD of the central $6'$ of NGC 6611 in Fig. 5. Within uncertainties, the least-massive stars already in the MS of NGC 6611 have mass in the range $3\text{--}5 M_\odot$.

Alternatively, we estimate the distance of NGC 6611 by means of the MS entry point of the PMS stars. To do this we use the turn-on locus in the reddening-corrected, field-star decontaminated CMD of the central $6'$ in Fig. 5. The PMS stars in Fig. 5 turn out to be basically contained within the 200 Kyr and 4 Myr isochrones (Siess et al. 2000), after applying an absolute distance modulus of $(m - M)_O = 11.09 \pm 0.30$. This corresponds to a distance from the Sun of $d_\odot = 1.65 \pm 0.27$ kpc which, within the uncertainties, agrees with the previous value based on the O V stars. For completeness we also show in Fig. 5 evolutionary tracks up to the zero-age main sequence (ZAMS) for PMS stars with masses 1, 2, 3 and $5 M_\odot$. Similarly to the value based on the 4 Myr Padova isochrone, the low-mass MS of NGC 6611 implied by the PMS occurs in the range $3\text{--}5 M_\odot$.

Based on the above estimates we adopt the average value $d_\odot = 1.8 \pm 0.5$ kpc as the distance of NGC 6611 from the Sun. With this value the Galactocentric distance of NGC 6611 turns out to be $d_{\text{GC}} = 6.3 \pm 0.5$ kpc, using 8.0 kpc as the distance of the Sun to the center of the Galaxy (Reid 1993). The present value

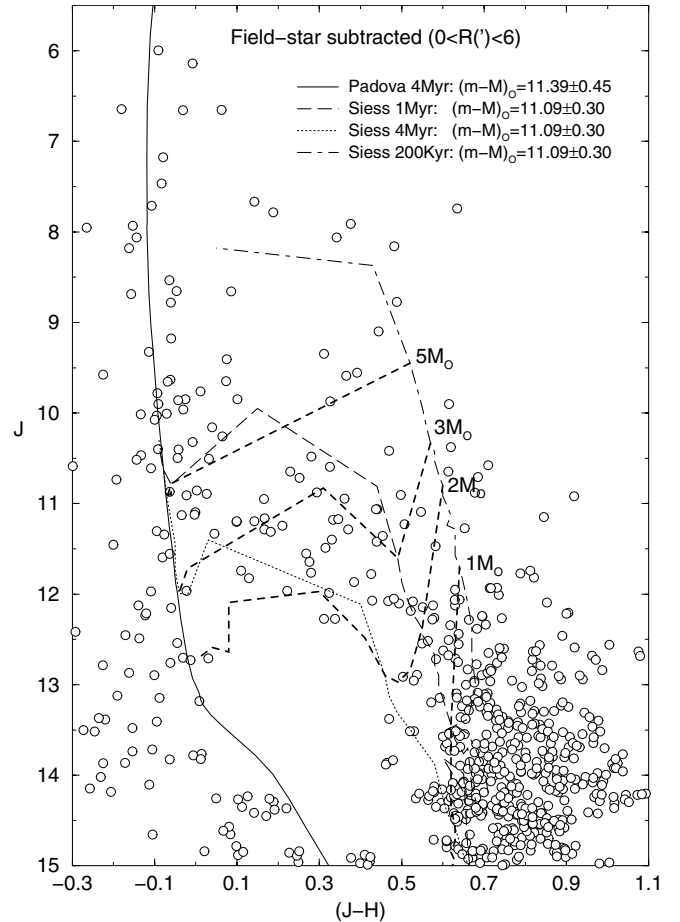


Fig. 5. The 4 Myr Padova isochrone set to the reddening-corrected, field-star decontaminated CMD of the central $6'$ of NGC 6611 according to $d_\odot = 1.92 \pm 0.45$ kpc. PMS model isochrones of Siess et al. (2000) with ages of 200 Kyr, 1 Myr and 4 Myr are fitted to the PMS population resulting in $d_\odot = 1.65 \pm 0.27$ kpc. Evolutionary tracks for PMS stars of masses 1, 2, 3 and $5 M_\odot$ are shown as dotted lines.

of the distance from the Sun agrees with that derived by Tadross et al. (2002) and is comparable to that of WEBDA (1.75 kpc), but falls ~ 0.5 kpc short with respect to the average value found in the literature.

4. Cluster structure

Structural parameters of NGC 6611 were derived by means of the radial density profile, defined as the projected number of stars per area around the cluster center. In the case of this low-latitude cluster the contamination of the CMD by field stars must be taken into account in order to derive the intrinsic radial distribution of stars. We do this by considering the colour-magnitude filter shown in the inset of Fig. 6 which, within uncertainties, describes the cluster CMD morphology from the upper MS to the PMS stars. Before counting stars we applied the colour-magnitude filter to the differential-reddening corrected CMD of the cluster (including stars with distance to the center from $0'$ to $23'$), to discard stars with discrepant colours. The colour-magnitude filtering procedure has been previously applied in the analysis of the open

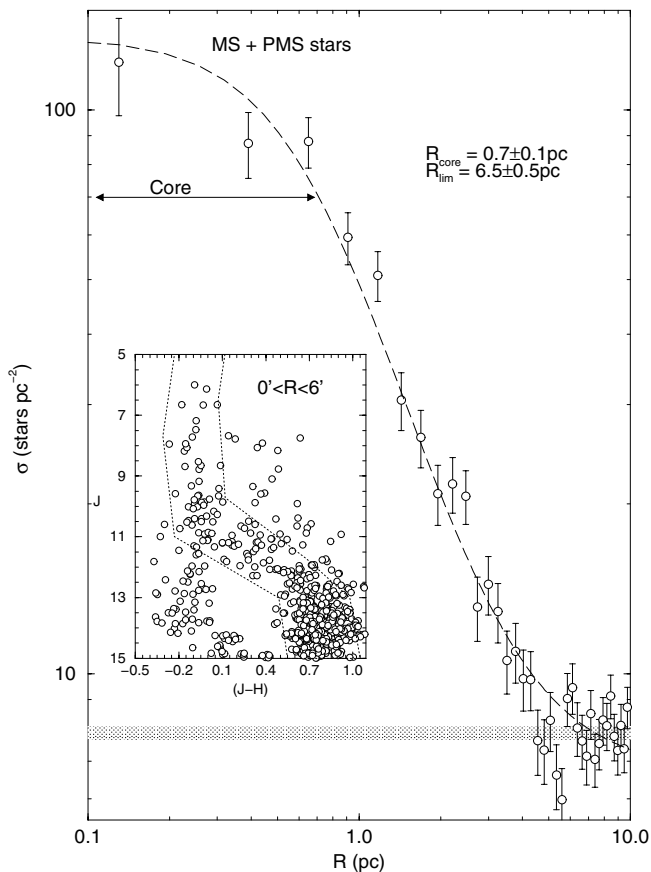


Fig. 6. Radial density profile of the cluster NGC 6611. Dashed line: 2-parameter King profile. Shaded region: stellar background level (average number of stars in the ring $17' \leq R \leq 22'$). The dimension of the core is indicated. The colour–magnitude filter used to discard stars with discrepant colours is shown in the inset, superimposed on the reddening-corrected and field-star decontaminated CMD of the central $6'$.

clusters M 67 (Bonatto & Bica 2003), NGC 188 (Bonatto et al. 2005) and NGC 3680 (Bonatto et al. 2004a). The radial density profile was obtained by counting stars inside concentric annuli with a step of $0.5'$ in radius. In the present case the background contribution level corresponds to the average number of stars included in the ring located at $17' \leq R \leq 22'$ ($8.8 \leq R(\text{pc}) \leq 11.4$), resulting in $\sigma_{\text{bg}} = 2.14 \pm 0.06 \text{ stars } (')^{-2} = 7.8 \pm 0.2 \text{ stars pc}^{-2}$. Note that the colour–magnitude filter encompasses both the MS and PMS stars.

The resulting radial density profile of the MS + PMS stars is shown in Fig. 6. For absolute comparison between clusters we scale the radius in the abscissa in parsecs, and the number density of stars in the ordinate in stars pc^{-2} using the distance derived in Sect. 3. The statistical significance of the profile is reflected in the 1σ Poisson error bars.

Structural parameters of NGC 6611 were derived by fitting the two-parameter King (1966a) surface density profile to the background-subtracted radial distribution of stars. The two-parameter King model essentially describes the intermediate and central regions of normal clusters (King 1966b; Trager et al. 1995). The fit was performed using a nonlinear least-squares fit routine which uses the errors as weights.

The best-fit solution is shown in Fig. 6 superimposed on the observed radial density profile. Parameters derived are the King background-subtracted central density of stars $\sigma_{0K} = 35 \pm 6 \text{ stars } (')^{-2} = 128 \pm 20 \text{ stars pc}^{-2}$, and the core radius $R_{\text{core}} = 1.35 \pm 0.15' = 0.7 \pm 0.1 \text{ pc}$. Considering the radial density profile fluctuations with respect to the background level, we can define a limiting radius (R_{lim}) for the cluster, in the sense that for regions beyond R_{lim} , the null-contrast between cluster and background star density would produce large Poisson errors and consequently, meaningless results. Thus, for practical purposes, the bulk of the cluster stars are contained within R_{lim} . For NGC 6611 we estimate a limiting radius $R_{\text{lim}} = 12.5 \pm 1.0' = 6.5 \pm 0.5 \text{ pc}$.

Despite the young age of NGC 6611 the King profile provides a good fit of the stellar content in this cluster, within uncertainties. Since it follows from an isothermal (virialized) sphere, the close similarity of the radial distribution of stars in NGC 6611 with a King profile may suggest that the internal structure of this cluster (particularly the core) has reached some level of energy equipartition. However, part of this effect appears to be related to formation processes as well (Sects. 5.2 and 6).

5. Luminosity and mass functions of the MS

The rather populous nature of NGC 6611 provides an opportunity to study the spatial distribution of LFs and MFs ($\phi(m) = \frac{dN}{dm}$) of the MS stars in such a young open cluster.

Based on the King profile fit of the MS radial density profile of NGC 6611 (Fig. 6) we decided to study the MF in the following regions: (i) $0.0 \leq R(\text{pc}) \leq 0.7$ (core), (ii) $0.7 \leq R(\text{pc}) \leq 6.5$ (halo), and (iii) $0.0 \leq R(\text{pc}) \leq 6.5$ (overall). In order to maximize the significance of background counts, we consider as offset field the outermost ring at $8.8 \leq R(\text{pc}) \leq 11.4$, which lies $\sim 2.3 \text{ pc}$ beyond the limiting radius.

Similarly to the structural analysis (Sect. 4) the first step in the present analysis is to take into account the field-star contamination. In this case we apply the colour–magnitude filter (Fig. 6) restricted to the MS stars (i.e. $J \leq 11.4$). The filtering process takes into account most of the field stars, leaving only a residual contamination. We deal with this residual contamination statistically by building LFs for each cluster region and offset field ($17' \leq R \leq 22'$) separately. We consider the three 2MASS bands independently when building the LFs. Note that the faint-magnitude limit of the MS is significantly brighter than that of the 99.9% Point Source Catalogue Completeness Limit (Sect. 3). We take $J = 5$ as the upper-MS limit (Fig. 3). We build the LF of each 2MASS band by counting stars in magnitude bins from the respective faint magnitude limit to the upper MS, both for each cluster region and offset field. Considering that the solid angle of the offset field may be different from that of a given cluster region, we multiply the offset field LF by a numerical factor so that the solid angles match. The intrinsic LF of each cluster region is obtained by subtracting the respective (i.e. solid angle-corrected) offset field LF from that of the cluster region. Finally, the intrinsic LFs are transformed into MFs using the mass-luminosity relation obtained from the 4 Myr Padova

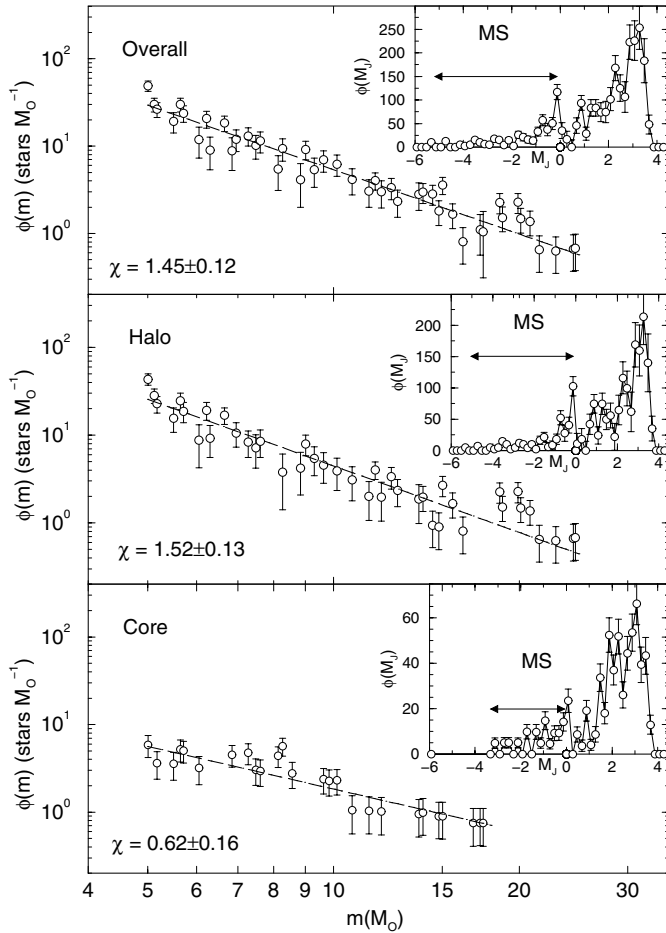


Fig. 7. Mass functions of the MS stars (empty circles) in different spatial regions of NGC 6611. Each panel contains MFs derived from the J , H and K_S 2MASS photometry. MF fits ($\phi(m) \propto m^{-(1+\chi)}$) are shown as dashed lines, and the respective MF slopes are given. The insets show the MS + PMS field-star subtracted LFs in each spatial region.

isochrone (the youngest one available) and the absolute distance modulus ($m - M_\odot = 11.39$ (Sect. 3)). These procedures are repeated independently for the three 2MASS bands. The final MF of a given cluster region is produced by combining the J , H and K_S MFs into a single MF. The resulting core, halo and overall MFs of NGC 6611, covering the mass range $5 \leq m(M_\odot) \leq 25$, are shown in Fig. 7. To these MFs we fit the function $\phi(m) \propto m^{-(1+\chi)}$. The resulting fits are shown in Fig. 7, and the MF slopes are given in Col. 4 of Table 1.

We show in each panel of Fig. 7 the corresponding field-star subtracted LFs, where the relative contribution of the PMS ($M_J \geq -0.12$) with respect to the MS can be evaluated.

Both the overall and halo MFs are slightly steeper than a typical Salpeter (1955) IMF ($\chi = 1.35$); however, the core MF turned out to be flat, with $\chi = 0.62 \pm 0.16$. The difference in MF slope between the core and halo ($\chi = 1.52 \pm 0.13$, panel b of Fig. 7), may be a consequence of mass segregation in the core. We discuss this point further in Sect. 5.2.

5.1. Total observed mass

We provide in Table 1 parameters derived from the MFs of each spatial region considered. The number of PMS stars in the core, halo and overall regions was estimated upon integration of the respective field star-subtracted LFs (Fig. 7) for $M_J \geq -0.12$. Considering the observed distribution of PMS stars and the respective evolutionary tracks (Fig. 5) and the fact that MFs in general increase in number for the subsolar-mass range, for simplicity we assume an average PMS mass of $1 M_\odot$. The resulting number and mass of PMS stars are in Cols. 2 and 3, respectively. The observed number of MS stars and corresponding mass (Cols. 5 and 6, respectively) are derived by integrating the MF through the mass range $5-25 M_\odot$. We add to these the corresponding values of the number and mass of PMS stars to derive the total number of observed stars (Col. 7), observed mass (Col. 8), projected mass density (Col. 9) and mass density (Col. 10).

To complete the census of the mass stored in observed stars in NGC 6611 we must include as well the stars more massive than $25 M_\odot$, which although present in the photometry, have not been counted in the mass estimate owing to the adopted MF upper cutoff ($25 M_\odot$). Hillenbrand et al. (1993) give the number of stars in selected mass bins for massive stars: 5 stars with mass in the range $25 \leq m(M_\odot) \leq 40$, 4 with $40 \leq m(M_\odot) \leq 60$, and 1 with $60 \leq m(M_\odot) \leq 85$. Accordingly, the mass stored in stars more massive than $25 M_\odot$ amounts to $\approx 435 M_\odot$, about 50% of the mass implied by the MF of the main sequence range considered above (Col. 6 of Table 1). For simplicity we add their mass to the overall region. To this effect we include an additional entry in Table 1 to account for the massive stars, resulting in $m_{\text{MS+PMS}} \sim 1630 M_\odot$. This value is ~ 4 times larger than the estimate of Tadross et al. (2002). The total observed mass of NGC 6611 is a factor ≈ 2 larger than the mass estimated for the Trapezium cluster (Lada & Lada 2003). It should be noted that the above mass and density estimates (Cols. (8)–(10) in Table 1) are in fact lower limits, since we are not taking into account stars less massive than $5 M_\odot$, a mass range for which we have no information on the behaviour of the MF slope.

5.2. Dynamical state of NGC 6611

The overall MF slope ($\chi = 1.45 \pm 0.12$) in the mass range $5 \leq m(M_\odot) \leq 25$ is similar to that of a standard Salpeter ($\chi = 1.35$) IMF. Besides, the MF slope presents large variations in the inner regions, being flat ($\chi = 0.62 \pm 0.16$) in the core and rather steep ($\chi = 1.52 \pm 0.13$) in the halo (Table 1 and Fig. 7). In older clusters this fact reflects the effects of large-scale mass segregation, in the sense that low-mass stars originally in the core are transferred to the cluster's outskirts while massive stars accumulate in the core. This produces a flat MF in the core and a steep one in the halo (see, e.g. Bonatto & Bica 2005).

Mass segregation in a star cluster scales with the relaxation time, defined as $t_{\text{relax}} = \frac{N}{8 \ln N} t_{\text{cross}}$, where $t_{\text{cross}} = R/\sigma_v$ is the crossing time, N is the (total) number of stars and σ_v is the velocity dispersion (Binney & Tremaine 1987). The characteristic time scale in which a cluster reaches some level of kinetic energy equipartition is described by t_{relax} , when massive stars

Table 1. Parameters derived from the MFs and PMS stars.

Region	PMS		Observed MS			Observed MS + PMS				τ
	N^*	m	χ_{5-25}	N^*	m_{obs}	N^*	$m_{\text{MS+PMS}}$	σ	ρ	
(pc)	(10^2 stars)	($10^2 M_{\odot}$)		(10^2 stars)	($10^2 M_{\odot}$)	(10^2 stars)	($10^2 M_{\odot}$)	($M_{\odot} \text{pc}^{-2}$)	($M_{\odot} \text{pc}^{-3}$)	
(1)	(2)	(3)	(4)	(5)	(6)	(7)	(8)	(9)	(10)	(11)
Core	1.0 ± 0.3	1.0 ± 0.3	0.62 ± 0.16	0.3 ± 0.2	2.3 ± 1.3	1.2 ± 0.4	4.1 ± 1.6	265 ± 107	284 ± 115	1.8 ± 0.6
Halo	2.6 ± 0.8	2.6 ± 0.8	1.52 ± 0.13	0.8 ± 0.3	6.9 ± 2.9	3.4 ± 0.9	9.6 ± 3.1	7.3 ± 2.3	0.83 ± 0.27	—
Overall	3.6 ± 1.2	3.6 ± 1.2	1.45 ± 0.13	0.9 ± 0.3	8.4 ± 3.2	4.5 ± 1.2	12.0 ± 3.4	9.0 ± 2.6	1.0 ± 0.3	0.067 ± 0.022
Overall [†]	3.6 ± 1.2	3.6 ± 1.2	1.45 ± 0.13	1.0 ± 0.3	12.7 ± 3.5	4.6 ± 1.3	16.3 ± 3.5	12.3 ± 2.6	1.4 ± 0.3	0.066 ± 0.022

Table Notes. Observed mass range: $5 - 25 M_{\odot}$. Column 4 gives the MF slope derived for the MS stars. Column 11: dynamical-evolution parameter $\tau = \text{age}/t_{\text{relax}}$. (†): includes stars more massive than $25 M_{\odot}$.

sink to the core and low-mass stars are transferred to the halo. Assuming a typical $\sigma_v \approx 3 \text{ km s}^{-1}$ (Binney & Merrifield 1998) we obtain for the overall cluster $t_{\text{relax}} \sim 20 \pm 5 \text{ Myr}$, and for the core $t_{\text{relax}} \sim 0.7 \pm 0.2 \text{ Myr}$. Considering that NGC 6611 is $\sim 1.3 \text{ Myr}$ old (Sect. 3), the age of this cluster is ~ 2 times larger than $t_{\text{relax}}(\text{core})$. Thus, the presence of mass segregation and consequently some degree of MF slope flattening can be expected in the core. However, the ratio cluster age to t_{relax} drops to ~ 0.07 for the overall cluster, which is consistent with the typical Salpeter slope and the absence of important mass segregation.

Although OB stars in NGC 6611 host more companions (for binaries with mass ratios $q \geq 0.1$) than solar-type field stars (Duchêne et al. 2001), the expected influence of binaries in the MF would be to steepen the slope of a standard Salpeter IMF to $\chi \approx 1.7$, and not to flatten it out (Sagar & Richtler 1991; Kroupa 2004).

6. Comparison with clusters in different dynamical-evolution states

In the previous sections we derived a series of parameters related to the structure and dynamical evolution of NGC 6611. At this point it may be useful to check how this young cluster fits in the context of open clusters with different ages and in more advanced dynamical states. Bonatto & Bica (2005) presented a systematic analysis of a set of open clusters with ages in the range $70 - 7000 \text{ Myr}$ and masses from $400 - 5300 M_{\odot}$. The methodology used follows the same lines as that used in the present paper. As a result, a set of uniform parameters related to the structure (core and overall radii, mass and density), dynamical state (core and overall MF slopes, evolutionary parameter $\tau = \text{age}/t_{\text{relax}}$), as well as age and Galactocentric distance of open clusters was obtained. Some correlations among these parameters were verified, and a separation of massive ($m \geq 1000 M_{\odot}$) and less-massive ($m \leq 1000 M_{\odot}$) clusters was observed. The core and overall dynamical-evolutionary parameter of NGC 6611 is given in Col. 11 of Table 1.

In Fig. 8 we compare NGC 6611 with the set of nearby, well-studied older clusters (Bonatto & Bica 2005) in terms of

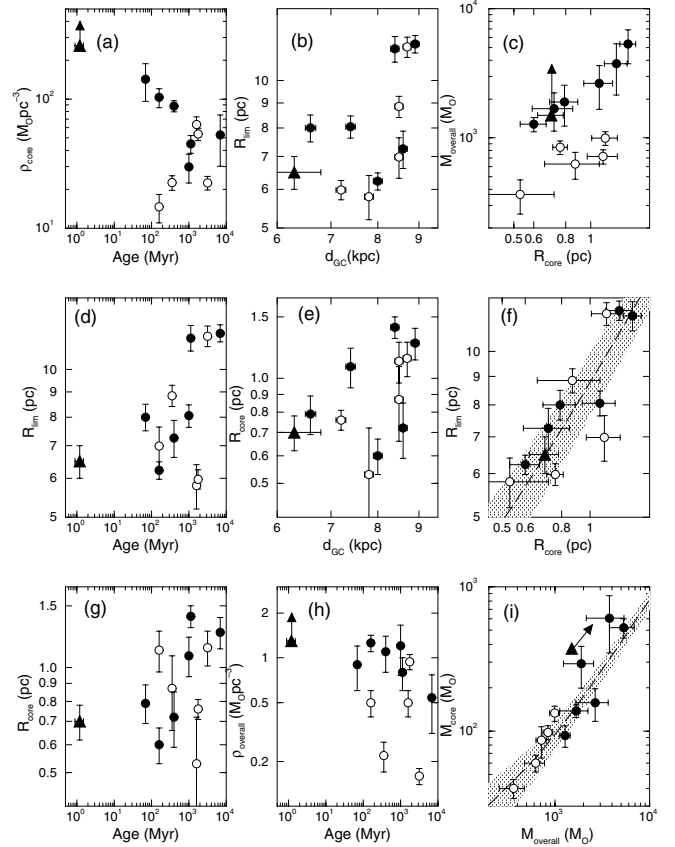


Fig. 8. Relations involving structural parameters of open clusters. Filled circles: clusters more massive than $1000 M_{\odot}$. Open circles, $m < 1000 M_{\odot}$. Filled triangle: NGC 6611. Dashed lines: least-squares fits to the nearby clusters (see text). Shaded areas: 1σ borders of the least-squares fits. Arrows indicate lower-limit estimates of mass and density for NGC 6611.

structural parameters. Note that the mass and density values of NGC 6611 are lower limits (Sect. 5.1). The limiting radius of NGC 6611 fits in the low-limit correlation of R_{lim} with age (panel d). Although with a larger scatter, the same is observed in the correlation of R_{core} with age (panel g). The core density of NGC 6611 follows the trend presented by massive clusters

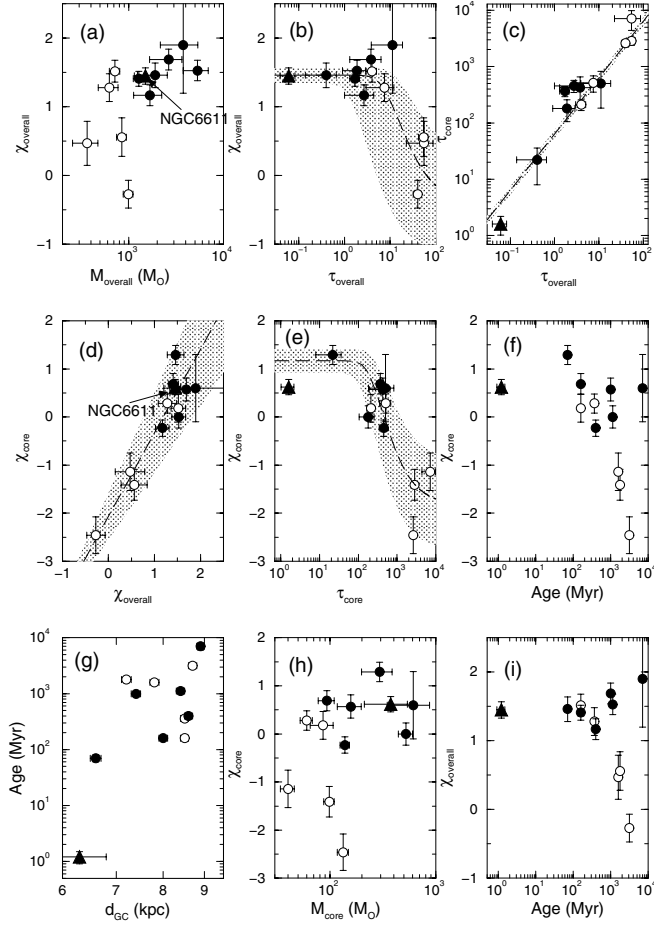


Fig. 9. Relations involving evolutionary parameters of open clusters. Symbols as in Fig. 8.

for young ages (panel a). A similar trend is seen for the overall density (panel h). In Galactocentric distance the limiting radius of NGC 6611 helps defining a correlation (panel b) in the sense that clusters at larger d_{GC} tend to be larger, which agrees with the results of Lyngå (1982) and Tadross et al. (2002). The large scatter in panel e precludes any conclusion with respect to a dependence of the core radius with d_{GC} . NGC 6611 fits well in the tight correlations of core and overall mass (panel i; least-squares fit: $M_{core} = (14.71 \pm 10.30) + (0.08 \pm 0.01)M_{overall}$ with a correlation coefficient $CC = 0.92$), and core and limiting radii (panel f; $R_{lim} = (1.05 \pm 0.45) + (7.73 \pm 0.66)R_{core}$ with $CC = 0.95$). Finally, in Bonatto & Bica (2005) we observed that massive and less-massive clusters follow parallel, different paths in the plane core radius \times overall mass. NGC 6611 consistently fits in the massive clusters path (panel c).

NGC 6611 is compared to older clusters in terms of dynamical-evolution related parameters in Fig. 9. NGC 6611 fits in the tight correlations of core and overall MF slopes (panel d; $\chi_{core} = (-2.07 \pm 0.46) + (1.74 \pm 0.35) \times \chi_{overall}$, with $CC = 0.87$), and core and overall evolutionary parameters (panel c; $\tau_{core} = (63.3 \pm 9.6) \times \tau_{overall}$, with $CC = 0.91$). The young age and small Galactocentric distance of NGC 6611 suggests a correlation of d_{GC} with age (panel g), which would agree with the result of Lyngå (1982). However, we note that this trend is mostly based on a single point (NGC 6611) and

thus, a larger cluster sample within the central sector is necessary to establish the statistical significance of the correlation. The Salpeter-like overall MF slope of NC 6611 is consistent with the overall mass and age relation when compared to other massive clusters (panels a and i, respectively). The scatter in panel h does not allow inferences on the relation of core MF slope with mass. Finally, with respect to the evolutionary parameters of NGC 6611, the overall MF slope (panel b; $\chi_{overall} = (1.5 \pm 0.1) - (1.9 \pm 0.6) \exp\left(-\frac{16.3 \pm 13.1}{\tau_{overall}}\right)$, with $CC = 0.89$) follows the relations suggested by massive clusters with small values of τ . However, the core MF slope is flatter than that expected for its value of τ (panel e; $\chi_{core} = (1.17 \pm 0.23) - (3.0 \pm 0.7) \exp\left(-\frac{439 \pm 156}{\tau_{core}}\right)$, with $CC = 0.82$) and age (panel f).

We conclude that both structurally and dynamically, the overall parameters of NGC 6611 fit in the relations defined by older, more-massive open clusters, in the loci expected of a very young cluster.

The core of NGC 6611 presents a MF significantly flatter than that in the halo, a situation typical of older clusters with important mass segregation. Part of this effect can be accounted for by the fact that the core relaxation time is about half the cluster age.

7. Concluding remarks

In this paper we analyzed the structure and mass distribution of MS and PMS stars in the ionizing open cluster NGC 6611. The analysis was based mostly on J , H and K_S 2MASS photometry corrected for the variable reddening across the region, from which we built radial density profiles and mass functions. The average colour excess in a region reaching $R \approx 23'$ from the center of NGC 6611 resulted in $E(J - H) = 0.25$, corresponding to $E(B - V) = 0.8$. To uncover the intrinsic CMD morphology we applied a field-star decontamination procedure to the reddening-corrected data. The resulting CMDs present a MS restricted to stars more massive than $\approx 5 M_{\odot}$ and a collection of PMS stars.

Based on the fraction of stars with K_S excess we estimated an age of $\sim 1.3 \pm 0.3$ Myr for NGC 6611. We derived a distance from the Sun of $d_{\odot} = 1.8 \pm 0.5$ kpc, considering the values calculated from O V stars with previous spectroscopic data and PMS tracks. Our value of d_{\odot} agrees with those given by Tadross (2002) and WEBDA. However, it locates NGC 6611 ~ 0.5 kpc closer to the Sun than the average value given in previous works. The direct method of distance determination using stars is fundamental for the definition of the Galactic structure. Note that available kinematic distances of the related H II region Sh2-49 are $d_{\odot} = 2.95$ kpc (Georgelin & Georgelin 1970) and $d_{\odot} = 2.2$ kpc (Blitz et al. 1982), thus larger than the present value.

King model fits to the radial density profiles including MS and PMS stars produced a core radius $R_{core} = 0.70 \pm 0.08$ pc with a limiting radius $R_{lim} \approx 6.5 \pm 0.5$ pc. The projected density of stars in the cluster center is $\sim 128 \pm 20$ stars pc^{-2} .

Considering the field star-subtracted LFs, we estimated that the number of PMS stars in NGC 6611 is ~ 362 . The total observed mass locked up in PMS and MS stars amounts to

$m_{\text{MS+PMS}} = (1.6 \pm 0.3) \times 10^3 M_{\odot}$. This is a lower-limit estimate since we are not taking into account stars less massive than $5 M_{\odot}$.

The core MF of the MS stars in NGC 6611 is flat with a slope $\chi = 0.62 \pm 0.16$, while in the halo it steepens to $\chi = 1.52 \pm 0.13$. The overall MF of NGC 6611 is similar to a Salpeter IMF with $\chi = 1.45 \pm 0.12$.

Compared to older open clusters in terms of structural and dynamical-evolution-related parameters, the overall cluster behaves as a massive open cluster at young ages.

The spatial variation of MF slopes, being flat in the core and steeper in the halo, implies that mass segregation has already affected the mass distribution in the core, since the relaxation time $t_{\text{relax}}(\text{core}) \sim 0.73 \text{ Myr}$ corresponds to $\sim 50\%$ of the cluster age. For the whole cluster $t_{\text{relax}}(\text{overall}) \sim 20 \text{ Myr} \sim 15 \times$ cluster age, which means that mass segregation did not have time to redistribute stars in large scale throughout the body of such a young cluster. Accordingly, the flattening degree in the core MF of NGC 6611 seems to be related as well to initial conditions, probably associated to the fragmentation of the parent molecular cloud itself, with more massive protostars preferentially located in the central parts of the cloud. This agrees with Kroupa (2004) with respect to the observed degree of mass segregation in clusters younger than a few Myr.

Acknowledgements. We are grateful to an anonymous referee for important remarks. This publication makes use of data products from the Two Micron All Sky Survey, which is a joint project of the University of Massachusetts and the Infrared Processing and Analysis Center/California Institute of Technology, funded by the National Aeronautics and Space Administration and the National Science Foundation. We also made use of the WEBDA open cluster database. We acknowledge support from the Brazilian Institutions CNPq and FAPEMIG.

References

- Alter, G., Ruprecht, J., & Vanisek, J. 1970, in *Catalogue of Star Clusters and Associations*, ed. G. Alter, B. Balázs, & J. Ruprecht
- Belikov, A. N., Kharchenko, N. V., Piskunov, A. E., & Schilbach, E. 1999, *A&AS*, 134, 525
- Belikov, A. N., Kharchenko, N. V., Piskunov, A. E., & Schilbach, E. 2000, *A&A*, 358, 525
- Binney, J., & Tremaine, S. 1987, in *Galactic Dynamics*, Princeton, NJ: Princeton University Press (Princeton series in astrophysics)
- Binney, J., & Merrifield, M. 1998, in *Galactic Astronomy* (Princeton, NJ: Princeton University Press, Princeton series in astrophysics)
- Blitz, L., Fich, M., & Stark, A. A. 1982, *ApJS*, 49, 183
- Bonatto, C., & Bica, E. 2003, *A&A*, 405, 525
- Bonatto, C. J., & Bica, E. 2005, *A&A*, 437, 483
- Bonatto, C. J., Bica, E., & Pavani, D. B. 2004a, *A&A*, 427, 485
- Bonatto, C., Bica, E., & Girardi, L. 2004b, *A&A*, 415, 571
- Bonatto, C. J., Bica, E., & Santos, Jr., J. F. C. 2005, *A&A*, 433, 917
- Bosch, G. L., Morrell, N. I., & Niemelä, V. S. 1999, *RMxAA*, 35, 85
- Chini, R., & Wargau, W. F. 1990, *A&A*, 227, 213
- Duchêne, G., Simon, T., Eislöffel, J., & Bouvier, J. 2001, *A&A*, 379, 147
- Dutra, C. M., Santiago, B. X., & Bica, E. 2002, *A&A*, 381, 219
- Georgelin, Y. P., & Georgelin, Y. M. 1970, *A&A*, 6, 349
- Girardi, L., Bertelli, G., Bressan, A., et al. 2002, *A&A*, 391, 195
- Greene, T. P., & Young, E. T. 1992, *ApJ*, 249, 481
- Greene, T. P., & Meyer, M. 1995, *ApJ*, 450, 233
- Gum, C. S. 1955, *MmRAS*, 67, 155
- Hester, J. J., Scowen, P. A., Sankrit, R., et al. 1996, *AJ*, 111, 2349
- Hillenbrand, L. A., Massey, P., Strom, S. E., & Merrill, K. M. 1993, *AJ*, 106, 1906
- Kenyon, S. J., & Hartmann, L. 1995, *ApJS*, 101, 117
- King, I. 1966a, *AJ*, 71, 64
- King, I. 1966b, *AJ*, 71, 276
- Kroupa, P. 2002, *Science*, 295, 82
- Kroupa, P. 2004, *New Astron. Rev.*, 48, 47
- Lada, C. J., & Lada, E. A. 2003, *ARA&A*, 41, 57
- Lada, C. J., Alves, J., & Lada, E. A. 1996, *AJ*, 111, 1964
- Lyngå, G. 1982, *A&A*, 109, 213
- Massey, P., Johnson, K. E., & Degioia-Eastwood, K. 1995, *ApJ*, 454, 151
- Mermilliod, J. C. 1996, in *The Origins, Evolution, and Destinies of Binary Stars in Clusters*, ed. E. F. Milone, & J.-C. Mermilliod, *ASP Conf. Ser.*, 90, 475
- Oliveira, J. M., Jeffries, R. D., van Loon, J. Th., Littlefair, S. P., & Naylor, T. 2005, *MNRAS*, submitted [arXiv:astro-ph/0501208]
- Reid, M. J. 1993, *ARA&A*, 31, 345
- Rodgers, A. W., Campbell, C. T., & Whiteoak, J. B. 1960, *MNRAS*, 121, 103
- Sagar, R., & Joshi, U. C. 1979, *A&AS*, 66, 3
- Sagar, R., Piskunov, A. E., Miakutin, V. I., & Joshi, U. C. 1986, *MNRAS*, 220, 383
- Sagar, R., & Richtler, T. 1991, *A&A*, 250, 324
- Schmidt-Kaler, T. 1982, in *Landolt-Börnstein, New Ser., Group VI*, (Springer-Verlag, Berlin), Vol. 2b, 1
- Salpeter, E. 1955, *ApJ*, 121, 161
- Sharpless, S. 1959, *ApJS*, 4, 257
- Siess, L., Dufour, E., & Forestini, M. 2000, *A&A*, 358, 593
- Skrutskie, M., Schneider, S. E., Stiening, R., et al. 1997, in *The Impact of Large Scale Near-IR Sky Surveys*, ed. Garzon et al., Kluwer (Netherlands), 210, 187
- Soares, J. B., & Bica, E. 2002, *A&A*, 388, 172
- Strom, K. M., Kepner, J., & Strom, S. E. 1995, *ApJ*, 438, 8130
- Tadross, A. L., Werner, P., Osman, A. & Marie, M. 2002, *NewAst*, 7, 553
- Thé, P. S., de Winter, D., Feinstein, A., & Westerlund, B. E. 1990, *A&AS*, 82, 319
- Trager, S. C., King, I. R., & Djorgovski, S. 1995, *AJ*, 109, 218
- Walker, M. F. 1961, *ApJ*, 133, 438
- Westerhout, G. 1958, *BAN*, 14, 215
- de Winter, D., Koulis, C., Thé, P. S., et al. 1997, *A&AS*, 121, 223